

Iron(II) and Copper(II) Complexes of HAPH,¹ a Bleomycin Metal Binding Site Analogue with Apical Imidazole Coordination

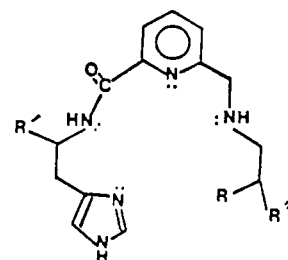
Thomas J. Lomis, Michael G. Elliott, Shirin Siddiqui, Maria Moyer, Richard R. Koepsel, and Rex E. Shepherd*

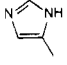
Received September 1, 1988

The analogue ligand HAPH for the metal ion binding site of bleomycin (BLM) has been synthesized and derivatized with Fe^{II} and Cu^{II}. HAPH has in-plane nitrogen donors of imidazole, deprotonated amide, pyridine, and secondary amine linked to a terminal, second imidazole moiety available for coordination. The last feature differs from a terminal amine in BLM. Visible spectra of Fe^{II}(HAPH) and Cu^{II}(HAPH) are similar to those of authentic Fe^{II}(BLM) and Cu^{II}(BLM), respectively. An electronic transition in the visible region, characteristic of the Fe^{II}(BLM) core chromophore, is observed to follow an order related to the ligand field strength and the axial donor: Fe^{II}(HAPH) (imidazole donor, 445 nm) > Fe^{II}(BLM) (amine donor, 465 nm) > Fe^{II}(SAPH-3) (sulfhydryl or H₂O donor, 475 nm) ≈ Fe^{II}(SAPH-1) (H₂O or -SCH₃ donor, 475 nm). E_{1/2} potentials for Fe^{III/II} couples (vs NHE) of Fe^{II}(HAPH) were found to depend on the pH and medium anions. In 0.10 M NaClO₄ at pH = 4, a reddish pink form has E_{1/2} = 0.47 V; the pH = 7 orange form has E_{1/2} = 0.407 V, and an orange-brown form produced at pH ≥ 8 has E_{1/2} = 0.092 V. The pH 7 form E_{1/2} value shifts to 0.457 V with 0.10 M NaCl added or to 0.067 V with 0.10 M phosphate buffer. The E_{1/2} value for Fe(HAPH)CO⁺ is 0.822 V in 0.10 M NaClO₄; the Fe^{II}(BLM) complexes gave E_{1/2} values of 0.092 V (phosphate), and its CO complex, Fe(BLM)CO, gave one of 0.937 V. Fe^{II}(HAPH)CO is formed reversibly with CO at 1.00 atm pressure with an approximate equilibrium constant of (5.4 ± 1.2) × 10³ M⁻¹; this shows that Fe^{II}(BLM) and its Fe(HAPH) analogue are capable of about 5.1 kcal/mol of back-donation to CO. Fe^{II}(HAPH) and Fe^{II}(BLM) were oxidized by O₂ in the presence of 0.24 M DMPO spin trap. Detection of a HODMPO[•] adduct in each case allowed the estimate of 53% efficiency for Fe^{II}(HAPH) compared to Fe^{II}(BLM) in generating HO[•] from coordinated O₂. When H₂O₂ (0.49 M) is used as the oxidant for Fe^{II}(HAPH), a 63% efficiency in forming HO[•] is recorded. The Cu^{II} derivatives of HAPH and BLM are shown to give frozen-glass ESR spectra similar to those of the reputedly pentacoordinate Cu^{II}(AMPHIS) and Cu^{II}(BLM) complexes. Cu^{II}(HAPH): λ_{max} = 570 nm, pH = 9.23; 50:50 DMSO/H₂O frozen glass at 77 K, g_{||} = 2.22, g_⊥ = 2.06, A_{||} = 201 × 10⁻⁴ cm⁻¹. Cu^{II}(BLM): λ_{max} = 590 nm, pH = 7.0; 50:50 DMSO/H₂O frozen glass at 113 K, g_{||} = 2.19, g_⊥ = 2.04, A_{||} = 189 × 10⁻⁴ cm⁻¹. Visible spectra of the Cu^{II}(HAPH) complex support an N₄ or N₅ coordination in aqueous solution above pH = 7.0 at room temperature.

Introduction

Bleomycins (BLM) are a family of antibiotic glycopeptides recognized as antitumor drugs used in the treatment of Hodgkin's lymphoma and carcinomas of the testis, head, skin, and neck.² The Fe^{II}(BLM) complex is an oxygen-sensitive species that is capable of mediating DNA strand scissions; the rapid activation of O₂ by Fe^{II}(BLM) is believed to account for the antitumor activity.³ The metal ion binding site of BLM contains the core donors of imidazole, deprotonated amide nitrogen, pyrimidine (pyridine-N), and secondary amine joined to a terminal primary amine. The last donor adopts the axial position, trans to the labile coordination site of O₂ binding. The structural features of Zn^{II}, Fe^{II}, Cu^{II}, and Co^{III} metallobleomycins have been studied previously by NMR, ESR, and X-ray diffraction methods.⁴ Synthetic methods have allowed the preparation of ligands that contain the core donors of bleomycin together with a choice in the terminal functional R group⁵⁻¹⁰ as shown in structure 1. These ligands



| | R | R' | R'' |
|--------|---|-----------------------|----------------------|
| AMPHIS | -NH ₂ | -C(O)OCH ₃ | H |
| PYML | -NH ₂ | -C(O)OH | -C(O)NH ₂ |
| HAPH |  | H | H |
| SAPH-1 | -SCH ₃ | H | H |
| SAPH-2 | -SCH ₂ C ₆ H ₄ OCH ₃ | H | H |
| SAPH-3 | -SH | H | H |

- (1) HAPH = N-(2-(imidazol-3-yl)ethyl)-6-(((2-(imidazol-3-yl)ethyl)-amino)methyl)-2-pyridinecarboxamide.
- (2) (a) Sugiura, Y.; Takita, T.; Umezawa, H. *Bleomycin Antibiotics: Metal Complexes and Their Biological Action. Metal Ions in Biological Systems*; Marcel Dekker: New York, 1985; Vol. 19, pp 81-108. (b) Umezawa, H. *Lloydia*, 1977, 40, 67. (c) Takita, T.; Muraoka, Y.; Nakatani, T.; Fujii, A.; Umezawa, Y.; Naganawa, H.; Umezawa, H. *J. Antibiot.* 1978, 31, 801. (d) Hecht, S. M. *Acc. Chem. Res.* 1986, 19, 383.
- (3) (a) Sausville, E. A.; Peisach, J.; Horwitz, S. B. *Biochem. Biophys. Res. Commun.* 1976, 73, 814. (b) Lown, J. W.; Sim, S. K. *Biochem. Biophys. Res. Commun.* 1977, 77, 1150. (c) Sausville, E. A.; Stein, R. W.; Peisach, J.; Horwitz, S. B. *Biochemistry* 1978, 17, 2746. (d) Takita, T.; Muraoka, Y.; Nakatani, T.; Fujii, A.; Itaka, Y.; Umezawa, H. *J. Antibiot.* 1978, 31, 1073. (e) Umezawa, H. *Prog. Biochem. Pharmacol.* 1976, 11, 18. (f) Stubbe, J.; Kozarich, J. W. *Chem. Rev.* 1987, 87, 1107.
- (4) (a) Oppenheimer, N. J.; Rodriguez, L. O.; Hecht, S. M. *Proc. Natl. Acad. Sci. U.S.A.* 1979, 76, 5616. (b) Lenkinski, R. E.; Dallas, J. L. *J. Am. Chem. Soc.* 1979, 101, 5902. (c) Tsukayama, M.; Randall, C. R.; Santillo, F. S.; Dabrowiak, J. C. *J. Am. Chem. Soc.* 1981, 103, 458. (d) Dabrowiak, J. C. *J. Inorg. Biochem.* 1980, 13, 317. (e) Dabrowiak, J. C.; Greenaway, F. T.; Santillo, F. S.; Crooke, S. T. *Biochem. Biophys. Res. Commun.* 1979, 91, 721. (f) Dabrowiak, J. C.; Tsukayama, M. *J. Am. Chem. Soc.* 1981, 103, 7543. (g) Itaka, Y.; Nakamura, H.; Nakatani, T.; Murata, Y.; Fujii, A.; Takita, T.; Umezawa, H. *J. Antibiot.* 1978, 31, 1070.

successfully model the bleomycin core in-plane donors and differ by the choice of the apical donor. Previous work has included studies of Fe^{II} and Cu^{II} complexes of PYML by Sugiura et al.⁵ and AMPHIS by Henichart et al.,⁶ which possess a terminal primary amine in the apical site.

- (5) Otsuka, M.; Yoshida, M.; Kobayashi, S.; Ohno, M.; Sugiura, Y.; Takita, T.; Umezawa, H. *J. Am. Chem. Soc.* 1981, 103, 6986.
- (6) (a) Henichart, J.-P.; Bernier, J.-L.; Houssin, R.; Lohez, M.; Kenani, A.; Cateau, J.-P. *Biochem. Biophys. Res. Commun.* 1985, 126, 1036. (b) Henichart, J.-P.; Houssin, R.; Bernier, J.-L.; Cateau, J.-P. *J. Chem. Soc., Chem. Commun.* 1982, 1295.
- (7) (a) Sugiura, Y. *J. Am. Chem. Soc.* 1980, 102, 5208. (b) Sugiura, Y.; Kuwahara, J.; Suzuki, T. *J. Chem. Soc., Chem. Commun.* 1982, 908. (c) Sugiura, Y.; Suzuki, T.; Kuwahara, J.; Tonaka, H. *Biochem. Biophys. Res. Commun.* 1982, 105, 1511.
- (8) Lomis, T. J.; Martin, J.; McCloskey, B.; Siddiqui, S.; Shepherd, R. E.; Siuda, J. F. *Inorg. Chim. Acta* 1989, 157, 99.
- (9) Lomis, T. J. M.S. Thesis, University of Pittsburgh, 1987 (University Microfilms: Ann Arbor, MI, 1987).
- (10) Lomis, T. J.; Siuda, J. F.; Shepherd, R. E. *J. Chem. Soc., Chem. Commun.* 1988, 290.

A fragment of the BLM core structure that contains the pyridine–amide–imidazole donors (PypepH) coordinated to Cu^{II} , Fe^{III} , and Co^{III} in the Pypep⁻ anion form has been prepared by Mascharak and co-workers.³⁴ A much improved PMAH model related to AMPHIS has been synthesized by Mascharak et al.⁴⁰ The $\text{Cu}^{\text{II}}(\text{PMA})^+$ complex, which has terminal amine–amine–pyrimidine–amide and imidazole donors, crystallizes as a five-coordinate distorted square pyramid.⁴⁰ The ESR parameters in a frozen glass nearly match those of $\text{Cu}^{\text{II}}(\text{AMPHIS})$.^{6,40}

$\text{Fe}^{\text{II}}(\text{BLM})$ is known to mimic a variety of the functions found in the cytochromes and heme metalloproteins.^{2,7} These include binding of O_2 ,⁴¹ and CO_2 and the formation of reactive oxygen species including O_2^- , HO^\bullet ,^{2,10} and ferryl oxygen^{35,41} much in the manner of various O_2 storage proteins, cytochrome P-450,³⁶ and catalase and peroxidase enzymes.^{2d} Analogues of the BLM core donor set that contain imidazole, sulfhydryl, or alkylated sulfur donors in the axial position would be closer to the hemes and cytochromes than the PYML, AMPHIS, or PMAH models. This aspect of the chemistry has been recently addressed by preparation of a series of terminal sulfhydryl and alkylated sulfur donors (SAPH-1–SAPH-3)^{8,9} and a terminal imidazole donor (HAPH).¹⁰ Details of the $\text{Fe}^{\text{II/III}}$ and Cu^{II} complexes with SAPH-1–SAPH-3 have been presented elsewhere.^{8–10} Although the active species of bleomycin action (HO^\bullet , O_2^- , $\text{Fe}^{\text{III}}\text{--O}$ atom, ferryl oxygen, etc.) is still in dispute, the ability of $\text{Fe}^{\text{II}}(\text{BLM})$ and its model complexes to generate trappable oxygen radical species has been used as one measure of the chemical activity of $\text{Fe}^{\text{II}}(\text{BLM})$ and its models.^{2,5,6} Typically the DMPO and PBN spin traps have been used to detect HO^\bullet or O_2^- .⁴⁸ $\text{Fe}^{\text{II}}(\text{SAPH-3})$, containing apical thiolato ($-\text{CH}_2\text{S}^-$) donation, is rapidly oxidized by O_2 , but no radicals, trappable by DMPO, escape the solvent cage.^{8,10} In contrast to the SAPH series, $\text{Fe}^{\text{II}}(\text{HAPH})$ exhibits an impressive ability to activate O_2 .¹⁰ $\text{Fe}^{\text{II}}(\text{HAPH})$ is 53% as efficient with O_2 as the oxidizing agent and 63% as efficient with H_2O_2 oxidant in forming HO^\bullet as the $\text{Fe}^{\text{II}}(\text{BLM})$ complex itself.¹⁰

$\text{Fe}^{\text{II}}(\text{HAPH})$ in the presence of O_2 and dithiothreitol induces DNA nicking of plasmid DNA with greater than 100-fold higher activity than $\text{Fe}(\text{edta})^{2-}/\text{O}_2$.³⁷ The $\text{Fe}^{\text{II}}(\text{HAPH})/\text{O}_2$ system also mediates the conversion of superhelical plasmid DNA into circular DNA as further evidence of DNA strand scissions.³⁷ Since $\text{Fe}(\text{edta})^{2-}/\text{O}_2$ has been used as a footprinting agent for DNA,³⁸ further studies of the coordination of Fe^{II} and Cu^{II} to HAPH are important for DNA footprinting and for potential antitumor drug design through selective modifications of one or more donors in the original BLM core. An important step in this direction has been made by Henichart and co-workers.⁴² The intercolating region from BLM-A₂ has been connected to the AMPHIS core model. This combination unit with Fe^{II} derivatization also successfully induced DNA strand scissions.⁴² Since AMPHIS has been shown to be less active inherently than HAPH,³⁷ further studies reported here of the metallo HAPH complexes will also be significant to this type of research.

Experimental Section

Synthesis of HAPH. The synthetic procedure is a modification of steps used in the synthesis of the SAPH ligand series.^{8–10} Histamine (0.22 g, 1.98 mmol) was dissolved in methanol (10 mL). Two drops of the indicator bromocresol purple (1% in methanol) was added to this solution. The solution was deep blue, indicating a basic pH. The pH was adjusted to 6 with the addition of 5 M HCl in methanol, as indicated by a yellow-green color. Size 3A molecular sieves were added to the flask. Methyl 2-formylpyridine-6-carboxylate^{5,9} (2; 0.30 g, 1.8 mmol) was then added to the mixture. The solution was stirred for 1.5 h with the pH maintained at 6. Sodium cyanoborohydride (0.09 g, 0.95 mmol) was then added, and the solution was stirred for 2 days. An additional amount of histamine (0.66 g, 5.9 mmol) was then added to the flask. The solution was dark blue, indicating a basic pH, which was not altered. After it was stirred for an additional 4 days, the solution was filtered and concentrated under vacuum to 1 mL. The reaction mixture was purified by preparative TLC ($\text{CHCl}_3/\text{C}_2\text{H}_5\text{OH}/\text{C}_2\text{H}_5\text{NH}_2$ (70% aqueous solution), 80:20:2) to yield the desired product, HAPH (0.365 g, 60% yield) as an oil (¹H and ¹³C NMR data below).⁴⁴

Synthesis of HAP. The procedure as outlined for the synthesis of HAPH was used to prepare 2-(((2-(imidazol-3-yl)ethyl)amino)-

methyl)pyridine (HAP) by the condensation of 0.21 g (2.00 mmol) of 2-pyridinecarboxaldehyde with 0.22 g (1.98 mmol) of histamine in methanol. Reduction was carried out with 0.09 g of NaBH_3CN . The separation of products was achieved by preparative TLC on silica gel, and the proper ¹H NMR spectrum (see below) was used to characterize the product.

$\text{Cu}^{\text{II}}(\text{HAPH})$ Complexes. $[\text{Cu}(\text{HAPH})](\text{ClO}_4)\cdot 1.61\text{H}_2\text{O}$ was isolated by procedures similar to those of Mascharak et al.⁴⁰ An FTIR spectrum that implicates the coordinated amide group of HAPH ($\nu_{\text{CO}} = 1574 \text{ cm}^{-1}$) is provided in the supplementary material as Figure SM-4.

Two methods were used to prepare suitable solutions of $\text{Cu}^{\text{II}}(\text{HAPH})$, with equivalent results. A weighed amount of HAPH (ca. 18 mg) was dissolved in 10.0 mL of water upon final dilution. A 0.885 M standard $\text{Cu}(\text{NO}_3)_2$ solution, prepared by dissolving electrochemically refined Cu wire, was pipetted into the HAPH solution such that 20% excess free ligand was present. The final concentration, based on Cu^{II} as the limiting reagent, was $4.41 \times 10^{-3} \text{ M}$. Adjustment of aliquots to desired pH values was made by the addition of concentrated NaOH or HCl while the pH was monitored at a combination glass/SCE minielectrode by an Fisher Accumet 801 pH meter.

The second method utilized the addition of an excess of standard Cu^{II} solution to form the 1:1 complex. The pH was raised to above 10, precipitating the excess Cu^{II} as the hydroxide. The insoluble $\text{Cu}(\text{OH})_2$ was removed filtration with Millipore filters of 0.47- μm mesh.¹¹ The filtered solution was adjusted to other desired pH values as described above. Samples for ESR study in 50:50 DMSO/water glasses were prepared by mixing a pH-adjusted solution with an equal volume of analytical grade DMSO prior to filling thin quartz ESR tubes for freezing in liquid nitrogen.

Fe^{II} Complexes. The preparations of $\text{Fe}^{\text{II}}(\text{HAPH})$, $\text{Fe}^{\text{II}}(\text{BLM})$, $\text{Fe}^{\text{II}}(\text{SAPH-3})$, and $\text{Fe}^{\text{II}}(\text{SAPH-1})$ solutions were similar. HAPH was synthesized as described in this work; BLM was the Bleoxane drug supplied by Bristol-Meyers Co. as a gift. SAPH-1 and SAPH-3 were prepared as in ref 8 and 9. A weighed amount of the desired ligand was dissolved in either 20.0 mL of H_2O or 20.0 mL of 0.05 M phosphate buffer ($\mu = 0.10$). These solutions were carefully purged of O_2 by means of bubbling Ar gas through the solutions in glass bubblers with necks sealed by rubber septa with use of standard gastight syringe methods. A glass/SCE minielectrode, calibrated against standard buffers, was mounted in a side neck of the flask containing the ligand solution. The Ar-purged solutions were deoxygenated by passage of the gas through Cr^{II} scrubbing towers and a prebubler water rinse tower. Weighed samples of $\text{Fe}(\text{NH}_4)_2(\text{SO}_4)_2\cdot 6\text{H}_2\text{O}$ were added to solutions of the ligands, which had been flushed with Ar for at least 20 min. A 5–10-min period was allowed for complexation and pH equilibration to take place. Fe^{II} was present as the limiting reagent such that there was a 20% excess of ligand. This method was used to assure that all Fe^{II} was bound as the desired ligand chelate and to accommodate any problems due to the hygroscopic nature of several of the synthetic ligands, the presence of nonstoichiometrically bound alcohols (present from the synthetic workup),⁴⁴ and the potential variability in the true effective molecular weight of BLM. Commercial BLM is a mixture of at least two species, which differ by the composition of a side-chain attachment; this functional group is not involved in the Fe^{II} binding, and the purification of the drug is not essential to its therapeutic use. An effective molecular weight of 1514, the weighted average of the forms present in Bleoxane, was used in concentration calculations.

The Fe^{II} complex solutions were adjusted to the desired pH by addition of concentrated, Ar-purged NaOH, by means of a 1.00-mL calibrated, gastight syringe. Aliquots were withdrawn by syringe methods and transferred to 1.00- or 2.00-cm Ar-purged quartz cells for UV-visible spectrophotometry or quartz flat cells after oxidation by O_2 or H_2O_2 for the ESR spin-trapping studies.

In studies involving CO complex formation, the Ar purging gas was temporarily replaced by bubbling CO (Air Products) through the Cr^{II} gas train. The entire assembly for Ar or CO purging was carried out in a hood with a strong exhaust system to remove the vented CO gas. Reversing the coordination of CO was carried out by vigorous Ar flushing for a period of 15 min; most of the $\text{Fe}^{\text{II}}(\text{HAPH})\text{CO}$, $\text{Fe}^{\text{II}}(\text{BLM})\text{CO}$, or $\text{Fe}^{\text{II}}(\text{SAPH-3})\text{CO}$ had disappeared within 12.0 min, as determined by the return of the tangerine or pink-orange color of these species.¹⁰ Total recovery of the initial complex was confirmed by matching initial and final visible spectra of the complexes.

ESR Spectra. Frozen-solution spectra¹² at 77 K were recorded at 9.019 GHz, 1.60-G modulation amplitude, and 20.0-mW power with 8.0-min scans and a 1.0-s time constant. Receiver gains (RG) are given

(11) Shepherd, R. E.; Hodgson, G. M.; Margerum, D. W. *Inorg. Chem.* **1971**, *10*, 989.

in the figure legends. ESR samples, prepared as described above, were kept in liquid N₂ inside of a quartz Dewar held in such a manner as to suspend the tube at the proper position in the microwave cavity of a Varian E-4 ESR spectrometer. The low-temperature ESR spectrum of Cu^{II}(BLM) at 113 K was obtained in the same frozen glass in a quartz ESR tube mounted in a Varian temperature controller unit within the cavity. Scanning parameters for Cu^{II}(BLM) at 8.85 × 10⁻³ M were 9.058-GHz microwave frequency, 6.3-G modulation amplitude, 20.0-mW power, 4.0-min scan, and 1.0-s time constant. The field was calibrated for all runs at room temperature with DPPH as the standard. Spin-trapping procedures using 5,5-dimethyl-1-pyrroline *N*-oxide (DMPO) were the same described previously by us.^{13-15,49}

UV-Visible Spectra. Spectra in the ultraviolet-visible region were obtained on solutions in 1.00- and 2.00-cm quartz glass cells at room temperature in the compartment of a Varian-Cary 118C spectrophotometer.

NMR Spectra. ¹H and ¹³C NMR data for the HAPH ligand were obtained on a JEOL FX90Q Fourier transform spectrometer: ¹H NMR (CD₃OD) δ 7.92, 7.87 (d, s, 2 H, im C₂H), 7.59 (m, 3 H, py ring H), 6.85 (d, 2 H, im C₅H), 3.98 (s, 2 H, py CH₂N), 3.65 (m, 2 H, im CH₂CH₂N) 2.9 (b, 6 H, im(1) CH₂, im(2) CH₂CH₂); ¹³C NMR (CD₃OD) δ 166.42 (CO), 157.76 (py C₂ (CO side)), 150.61 (py C₆), 139.39 (py C₄), 136.19 (im C₂ and C₄), 126.41 (py C₅), 121.73 (py C₃), 117.94, 117.45 (im C₅), 53.90 (py CH₂N), 51.79 (COCH₂py), 50.87 (Imid(2) NHCH₂CH₂-im(2)), 49.89, 49.46 (CH₂-im(1), CH₂-im(2)). Assignments are based on those for the related AMPHIS and SAPH series, which are described in detail elsewhere.^{6,8,9}

¹H NMR data for HAP (CD₃OD): δ 8.50 (d, 1 H, im C₂H), 7.80, 7.58, 7.42, 7.21 (t, s, d, d, total 4 H, py ring H), 6.87 (s, 1 H, im C₅H), 3.92 (s, 2 H, py CH₂N), 2.89 (t, 4 H, NCH₂CH₂-im).

Mass Spectral Data. A high-resolution mass spectrum of the HAPH ligand was obtained (HRMS (*m/z*): found, 339.1806; calcd, 339.1808) with a Varian V6 70-G double-focusing mass spectrometer. Other MS peaks (*m/z*) are 339 (M⁺, 22%), 258 (82%), 230 (100%), and 95 (98%).

Electrochemical Methods. Redox potentials were measured with an IBM EC/225 voltammetric analyzer in the differential pulse (DP) and cyclic voltammetry (CV) modes. A pulse amplitude of 50 mV at a sweep rate of 10 mV/s was employed for DP; scan rates of 100 mV/s were typical for CV data. A three-electrode system consisting of a glassy-carbon working electrode, a sodium chloride saturated calomel reference electrode (SSCE), and a Pt-wire auxiliary electrode was used. Calibration with the reversible one-electron wave of Ru(NH₃)₆Cl₃ is described elsewhere.⁸

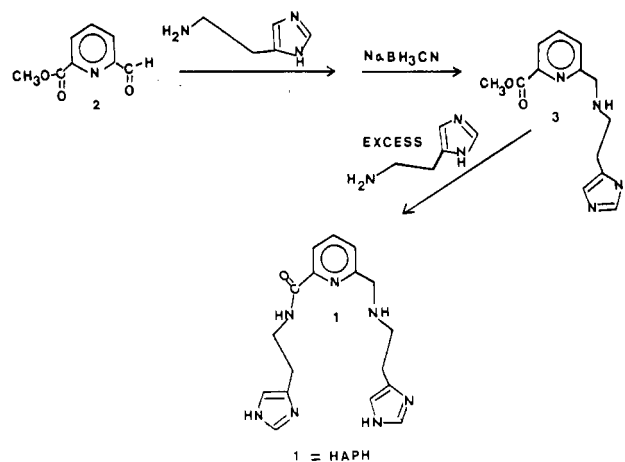
The solvent, deoxygenated with N₂, consisted of pH = 6.86 phosphate buffer (μ = 0.10), 0.10 M NaClO₄, or 0.10 M NaClO₄ plus 0.10 M NaCl. The weighed ligand was added to the deoxygenated solvent to achieve a molarity of (1–6) × 10⁻³ M. A preweighed amount of Fe(II) as Fe(NH₄)₂(SO₄)₂·6H₂O was added such that the ligand was in about 17% excess. The potential range was scanned immediately and then scanned at appropriate subsequent intervals up to 150 min.

Reversible CO binding by these complexes was studied by a somewhat different technique. CO adducts of the Fe(II) complexes (10⁻³ M) were prepared in bubblers as described above and transferred to the N₂-purged electrochemical cell by standard syringe techniques. A N₂ atmosphere was maintained over the solution while the differential pulse polarograph was recorded. Bubbling these solutions with N₂ for ~10 min allowed the decay of the CO complex to be studied. A similar experiment was performed with CV. CO was bubbled through the electrochemical cell until a significant CV wave for the Fe(HAPH)CO complex was detected together with the Fe(HAPH)(H₂O) species. Reversibility was shown by an N₂ purge, which allowed recording of a CV trace matching the one prior to CO admission to the cell. These data are shown in Figure 3, where the additional wave for the partially formed CO complex is clearly observed in sweep 2 while only the aqua complex is present before and after admission of CO followed by the N₂ purge (before CO, sweep 1; after N₂ purge, sweep 3).

Results and Discussion

Synthesis of HAPH. The synthesis of HAPH (structure 1) was accomplished as described in the Experimental Section (Scheme I). Proper ¹H and ¹³C NMR and high-resolution mass spectral data given in the Experimental Section confirm the structure of the isolated HAPH molecule. The X-ray structure of [Cu(HAPH)](ClO₄)·1.61H₂O proves the connectivity of the HAPH ligand.³⁷ The ligand HAP, which has the same structure as intermediate 3 in Scheme I, minus the methyl ester of the carboxylic acid, was also prepared in order to provide the pyridine-amine-imidazole linkage for comparison with HAPH as a ligand donor.

Scheme I

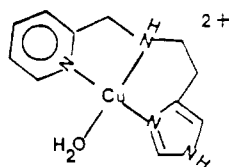


Cu^{II}(HAPH) and Cu^{II}(HAP) Complexes. When Cu^{II}(HAPH) is prepared at pH = 3.18, the solution is pale blue (λ_{max} = 630 nm, ε = 145 M⁻¹ cm⁻¹; Figure SM1, SM = supplementary material). The spectrum shifts to a new maximum at 570 nm (ε = 132 M⁻¹ cm⁻¹) above pH = 7, indicative of deprotonated amide coordination; the solution appears bluish purple. The pK_a value for this change is 6.50 ± 0.05, as determined from a spectrophotometric titration (22 °C, μ = 0.013). This equilibrium does not occur at a pH suitable for deprotonation of the pyrrole NH of the imidazole moieties; for example Cu(dien)(imH)²⁺ exhibits a pK_a value above 10.^{12,17} The only titratable group is the re-

- (12) Siddiqui, S.; Shepherd, R. E. *Inorg. Chem.* **1986**, *25*, 3869.
- (13) Myser, T. K.; Shepherd, R. E. *Inorg. Chem.* **1987**, *26*, 1544.
- (14) (a) Johnson, C. R.; Myser, T. K.; Shepherd, R. E. *Inorg. Chem.* **1988**, *27*, 1089. (b) Shepherd, R. E.; Myser, T. K.; Elliott, M. G. *Inorg. Chem.* **1988**, *27*, 916.
- (15) Johnson, C. R.; Shepherd, R. E. In *Mechanistic Aspects of Inorganic Chemistry*; ACS Symposium Series 198, Rorabacher, D. B., Endicott, J. F., Eds.; American Chemical Society: Washington, DC, 1982.
- (16) The geometry is implicated by the axial ESR spectrum together with the required lowering of symmetry due to the chelate linkage for the N-donors of differing type.
- (17) O'Young, C. L.; Dewan, J. C.; Lillenthal, H. R.; Lippard, S. J. *J. Am. Chem. Soc.* **1978**, *100*, 7291.
- (18) Bates, R. G. *Determination of pH*; Wiley: New York, 1964.
- (19) (a) Kivelson, D.; Nieman, R. *J. Chem. Phys.* **1961**, *35*, 157. (b) Gersmann, H. R.; Swalen, J. D. *J. Chem. Phys.* **1962**, *36*, 322. (c) Wiersema, A. K.; Windle, J. J. *J. Phys. Chem.* **1964**, *68*, 2316.
- (20) (a) Bonomo, R. P.; Riggi, F. *Chem. Phys. Lett.* **1982**, *93*, 99. (b) McGarvey, B. R. *Transition Met. Chem. (N.Y.)* **1966**, *3*, 89.
- (21) Shepherd, R. E.; Proctor, A.; Henderson, W. W.; Myser, T. K. *Inorg. Chem.* **1987**, *26*, 2440.
- (22) Melnyk, D. L.; Horwitz, S. B.; Peisach, J. *Biochemistry* **1981**, *20*, 5327.
- (23) Isied, S. S.; Taube, H. *Inorg. Chem.* **1976**, *15*, 3070.
- (24) (a) Johnson, C. R.; Shepherd, R. E.; Marr, B.; O'Donnell, S.; Dressich, W. *J. Am. Chem. Soc.* **1980**, *102*, 6227; (b) Johnson, C. R.; Shepherd, R. E. *Inorg. Chem.* **1983**, *22*, 3506. (c) Sabo, E. M.; Shepherd, R. E.; Rau, M. S.; Elliott, M. G. *Inorg. Chem.* **1987**, *26*, 2897.
- (25) (a) Janzen, E. G. *Acc. Chem. Res.* **1971**, *4*, 31. (b) Evans, C. A. *Aldrichim. Acta* **1979**, *12*, 23.
- (26) Wishart, J. F.; Taube, H.; Breslau, K. J.; Isied, S. *Inorg. Chem.* **1984**, *23*, 2997.
- (27) Siddiqui, S.; Henderson, W. W.; Shepherd, R. E. *Inorg. Chem.* **1987**, *26*, 3101.
- (28) Johnson, C. R.; Shepherd, R. E. *Inorg. Chem.* **1983**, *22*, 1117.
- (29) (a) Lim, H. S.; Barclay, D. J.; Anson, F. *Inorg. Chem.* **1972**, *11*, 1460. (b) Kuehn, C.; Taube, H. *J. Am. Chem. Soc.* **1976**, *98*, 689. (c) Reference 23.
- (30) Johnson, C. R.; Shepherd, R. E. *Synth. React. Inorg. Met.-Org. Chem.* **1984**, *14*, 339.
- (31) (a) Sugiura, T.; Suzuki, M.; Otsuka, S.; Kobayashi, M.; Ohno, M.; Takita, T.; Umezawa, H. *J. Biol. Chem.* **1983**, *258*, 1328. (b) Dabrowiak, J. C.; Greenaway, F. T.; Longo, W. F.; Van Husen, M.; Crooke, S. T. *Biochim. Biophys. Acta* **1978**, *517*, 517.

maining amide functionality or coordinated water. Changing a coordinated H_2O to OH^- on Cu^{II} does not promote a major change in ligand field. Therefore, the pH-dependent effect is due to amide deprotonation, which is known to occur at $\text{pH} = \text{ca. } 5\text{--}8$ for Cu^{II} complexes.^{16,45} These changes are similar to the switch from N_3O to N_4 (or N_5) coordination upon addition of an imidazole donor to $\text{Cu}(\text{dien})(\text{H}_2\text{O})^{2+}$ ($\lambda_{\text{max}} = 619 \text{ nm}$): $\text{Cu}(\text{dien})(\text{imH})^{2+}$, $\lambda_{\text{max}} = 580 \text{ nm}$; $\text{Cu}(\text{dien})(\text{imH})_2^{2+}$, $\lambda_{\text{max}} = 582 \text{ nm}$.¹²

$\text{Cu}(\text{HAP})(\text{H}_2\text{O})^{2+}$ was prepared at a $2.41 \times 10^{-2} \text{ M}$ concentration to obtain additional evidence concerning the spectral changes of $\text{Cu}^{\text{II}}(\text{HAPH})$ with pH. The spectrum of $\text{Cu}^{\text{II}}(\text{HAPH})$ is shown in Figure 1.



$(\text{HAP})(\text{H}_2\text{O})^{2+}$ was examined from $\text{pH} = 4.13$ to $\text{pH} = 9.82$. In the pH regime below 5.20 the spectrum of $\text{Cu}(\text{HAP})(\text{H}_2\text{O})^{2+}$ is consistent with the N_3O ligand field of pyridine–amine–imidazole–water donors ($\lambda_{\text{max}} = 630 \text{ nm}$, $\epsilon = 44 \text{ M}^{-1} \text{ cm}^{-1}$, similar to $\text{Cu}(\text{dien})(\text{H}_2\text{O})^{2+}$, $\lambda_{\text{max}} = 619 \text{ nm}$). Increasing the pH above 5.20 produces an intensity increase ($\epsilon \approx 56 \text{ M}^{-1} \text{ cm}^{-1}$) but no shift in λ_{max} up to $\text{pH} = 7.50$. The intensity change is attributed to deprotonation of coordinated water ($\text{p}K_a \approx 6.3$), forming $\text{Cu}(\text{HAP})(\text{OH})^+$, which retains the N_3O ligand field. A new species is observed in 0.12 M imidazole/0.18 M imidazolium ion buffer ($\text{pH} = 6.84$) or 0.098 M imidazole ($\text{pH} = 9.43$). This species has a visible spectral maximum at 588 nm, only slightly above the wavelength of the d–d band produced by the N_4 donor set of $\text{Cu}(\text{dien})(\text{imH})^{2+}$; $\lambda_{\text{max}} = 580 \text{ nm}$. Therefore, the anticipated $\text{Cu}(\text{HAP})(\text{imH})^{2+}$ species is detected. Addition of free imidazole at 0.20 M ($\text{pH} 9.78$) promotes formation of another species with λ_{max} at 598 nm. The lower ligand field at higher [imH] suggests formation of a five-coordinate species, $\text{Cu}(\text{HAP})(\text{imH})_2^{2+}$.

The results with $\text{Cu}(\text{HAP})(\text{H}_2\text{O})^{2+}$ and its imidazole adducts have several implications concerning the coordination modes of $\text{Cu}^{\text{II}}(\text{HAPH})$. $\text{Cu}^{\text{II}}(\text{HAPH})$ exhibits the same ligand field at $\text{pH} = 3.81$ as $\text{Cu}(\text{HAP})(\text{H}_2\text{O})^{2+}$. The chelation of $\text{Cu}^{\text{II}}(\text{HAPH})$ must then be N_3O and presumably shares the coordinated portion of HAPH that is available in HAP. This means that the imidazole moiety adjacent to the amide is pendant. At $\text{pH} 3.18$ the pendant imidazole will be partially protonated. Its $\text{p}K_a$ was found to be ca. 3.0 by titration and compares favorably with the value of ca. 3.4 for the similar structure adopted by the $\text{M}^{\text{II}}(4\text{-IMDIEN})$ complexes of Martell et al.³⁹ Martell has measured $\log K_{\text{MHL}}$

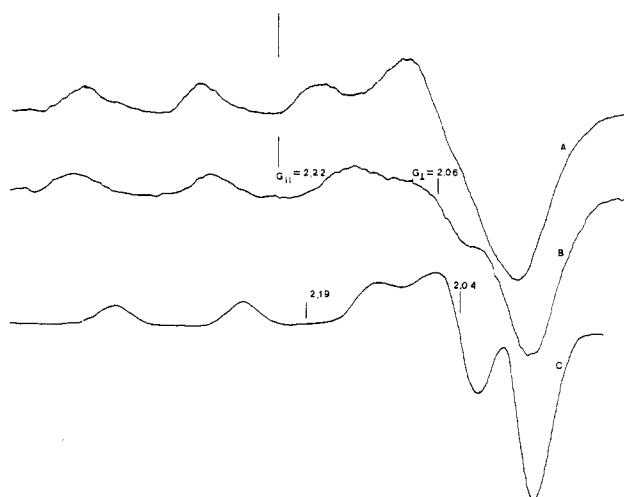
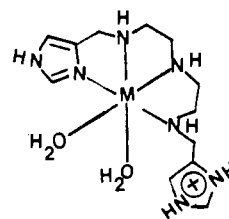


Figure 1. ESR spectra of $\text{Cu}^{\text{II}}(\text{HAPH})$ and $\text{Cu}^{\text{II}}(\text{BLM})$ in $\text{Me}_2\text{SO}/\text{water}$ glasses: (A) $[\text{Cu}(\text{HAPH})] = 2.20 \times 10^{-3} \text{ M}$, $\text{pH} = 3.50$, 77 K , $\text{RG} = 8.0 \times 10^3$ (other parameters are given in the Experimental Section); (B) $[\text{Cu}(\text{HAPH})] = 2.20 \times 10^{-3} \text{ M}$, $\text{pH} = 9.56$, 77 K , $\text{RG} = 8.0 \times 10^3$; (C) $[\text{Cu}(\text{BLM})] = 8.85 \times 10^{-3} \text{ M}$, $\text{pH} = 7.0$, 113 K , $\text{RG} = 3.2 \times 10^2$.

values of 3.35 for Cu^{II} and 3.30 for Co^{II} with 4-IMDIEN.³⁹ The Cu^{II} complex of 4-IMDIEN should be nearly square planar due to the Jahn–Teller distortion; the other complexes coordinate as shown by Martell et al.³⁹



At $\text{pH} \geq 6.50$, the spectrum of $\text{Cu}^{\text{II}}(\text{HAPH})$ shifts to 570 nm upon amide deprotonation. This ligand field is greater than the N_4 field provided by $\text{Cu}(\text{HAP})(\text{imH})^{2+}$ (e.g. 588 nm). This stronger ligand field is consistent with amide coordination in this range.⁴⁵ The ligand field provided by pyridine–amine–imidazole–water in $\text{Cu}(\text{HAP})(\text{H}_2\text{O})^{2+}$ is weaker than the pyridine–amide–imidazole–water field of $\text{Cu}(\text{Pyep})(\text{H}_2\text{O})^+$,³⁴ $\text{Cu}(\text{HAP})(\text{H}_2\text{O})^{2+}$ appears at 15 nm lower energy (630 vs 615 nm³⁴). One would predict an N_4 ligand field of in-plane imidazole-deprotonated amide–pyridine and amine to form a Cu^{II} complex with a d–d spectral transition at 571 nm for $\text{Cu}^{\text{II}}(\text{HAPH})$. Coordination of the fifth axial imidazole donor ought to increase the wavelength to ca. 577 nm. The observed maximum for $\text{Cu}^{\text{II}}(\text{HAPH})$ at $\text{pH} \geq 7.0$ of 570 nm supports four in-plane N donors, one being the deprotonated amide. Coordination of the amide places its nearby imidazole close enough to form a six-membered chelate ring. The proximity effect of a pendant imidazole above $\text{pH} = 7.0$ favors the N_5 coordination, particularly at lower temperature.¹² The similarity of the ESR spectra of $\text{Cu}^{\text{II}}(\text{BLM})$ and

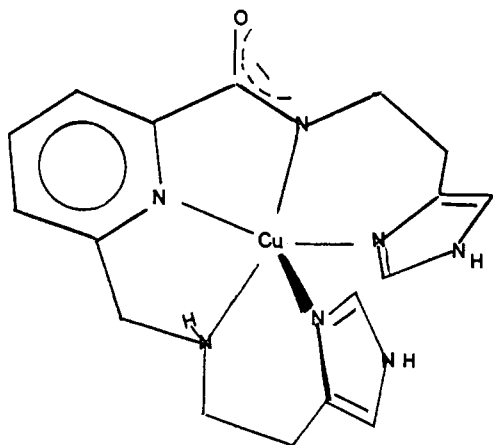
- (32) (a) Collman, J. P.; Brauman, J. I.; Doxsee, K. M.; Sessler, J. L.; Morris, R. M.; Gibson, Q. H. *Inorg. Chem.* **1983**, *22*, 1427 and references therein. (b) Chang, C. K.; Traylor, T. G. *Proc. Natl. Acad. Sci. U.S.A.* **1975**, *72*, 1166 and references therein. (c) Collman, J. P.; Halbert, T. R.; Suslick, K. S. In *Metal Ion Activation of Dioxygen*; Spiro, T. G., Ed.; Wiley: New York, 1980; Chapter 1.
- (33) (a) Sweigart, D. A.; O'Brien, P. *Inorg. Chem.* **1985**, *24*, 1405. (b) Doeff, M. M.; Sweigart, D. A.; O'Brien, P. *Inorg. Chem.* **1983**, *22*, 851.
- (34) (a) DeIany, K.; Arota, S. K.; Mascharak, P. K. *Inorg. Chem.* **1988**, *27*, 705. (b) Tao, X.; Stephan, D. W.; Mascharak, P. K. *Inorg. Chem.* **1987**, *26*, 754. (c) Brown, S. J.; Tao, X.; Stephan, D. W.; Mascharak, P. K. *Inorg. Chem.* **1986**, *25*, 3377.
- (35) Burger, R. M.; Peisach, J.; Horowitz, S. B. *J. Biol. Chem.* **1981**, *256*, 11636.
- (36) Coon, M. J.; White, R. E. *Metal Ion Activation of Dioxygen*. In *Metal Ions in Biology*; Spiro, T. G., ed.; Wiley: New York, 1980; Vol. 2, Chapter 2. (b) See also reviews in ref 2a,d.
- (37) Lomis, T. J.; Shepherd, R. E.; Hedge, R.; Mistry, J. S.; Koepsel, R. R. Submitted for publication in *J. Am. Chem. Soc.*
- (38) (a) Tullius, T. D.; Dombroski, B. A. *Science* **1985**, *230*, 679. (b) Hertzberg, R. P.; Dervan, P. B. *J. Am. Chem. Soc.* **1982**, *104*, 313.
- (39) Timmons, J. H.; Harris, W. R.; Murase, I.; Martell, A. E. *Inorg. Chem.* **1978**, *17*, 2192.
- (40) (a) Brown, S. J.; Mascharak, P. K.; Stephan, D. W. *J. Am. Chem. Soc.* **1988**, *110*, 1996. (b) Brown, S. J.; Hudson, S. E.; Stephan, D. W.; Mascharak, P. K. *Inorg. Chem.* **1989**, *28*, 468.
- (41) Burger, R. M.; Horowitz, S. B.; Peisach, J.; Wittenberg, J. B. *J. Biol. Chem.* **1979**, *254*, 12299.
- (42) (a) Kenani, A.; Lohez, M.; Houssin, R.; Helbecque, N.; Bernier, J.-L.; Lemay, P.; Henichart, J. P. *Anti-Cancer Drug Des.* **1987**, *2*, 47. (b) Bailly, C.; Chateau, J.-P.; Hebecque, N.; Bernier, J.-L.; Houssin, R.; Denis, C.; Henichart, J. P. *J. Inorg. Biochem.* **1987**, *31*, 211.
- (43) Shepherd, R. E. *J. Am. Chem. Soc.* **1976**, *98*, 3329.
- (44) ¹H NMR and ¹³C NMR data showed the absence of other organic products or materials other than HAPH and bound $\text{C}_2\text{H}_5\text{OH}$ and $\text{C}_2\text{H}_5\text{NH}_2$ from the chromatographic separation. The chromatographic agents are strongly H-bonded to HAPH. These agents came off very slowly under high vacuum over 8 h. Their presence in the isolated oil makes elemental analysis of little value in comparison to the more sophisticated techniques of NMR and high-resolution mass spectrometry.
- (45) Sigel, H.; Martin, R. B. *Chem. Rev.* **1982**, *82*, 385.

Table I. UV-Visible Absorption Maxima of HAPH, SAPH-1, SAPH-3, and BLM Complexes

| complex | pH | λ_{\max} , nm | ϵ , M ⁻¹ cm ⁻¹ | ref ^a |
|-----------------------------|------|-----------------------|---|------------------|
| Fe ^{II} (HAPH) | 7.75 | 445 | 278 | |
| Fe ^{II} (HAPH)CO | 7.50 | 360, 390 | 837 ± 30 | |
| Fe ^{III} (HAPH) | 7.75 | ~400 ^b | (610) ^b | |
| Fe ^{II} (BLM) | 8.20 | 465 | 365 | |
| Fe ^{II} (BLM) | 6.10 | 476 | 380 | 2a,c |
| Fe ^{II} (BLM)CO | 6.90 | 405 | 947 ^c | |
| Fe ^{II} (SAPH-3) | 6.88 | 475 | 133 | |
| Fe ^{II} (SAPH-3) | 8.00 | 475 | 200 ± 10 | |
| Fe ^{II} (SAPH-3)CO | 6.75 | 400, 390 | 522 ^c | |
| Fe ^{III} (SAPH-3) | 6.88 | 475 ^b | (268) ^b | |
| Fe ^{II} (SAPH-1) | 8.00 | 475 | 410 | |
| Fe ^{III} (SAPH-1) | 8.00 | ~475 | (285) ^b | |
| Fe ^{II} (PYML) | 6.8 | 465 | 300 | 5 |
| Fe ^{II} (PYML)CO | 6.8 | 390 | 2000 | |
| Cu ^{II} (HAPH) | 3.18 | 630 | 145 | |
| Cu ^{II} (HAPH) | 9.23 | 570 | 132 | |
| Cu ^{II} (BLM) | 7.00 | 590 | 72 | |
| Cu ^{II} (PYML) | 6.8 | 595 | 120 | 5 |

^aThis work unless specified; $T = 22$ °C. ^bFe^{III} complexes are metastable; cloudiness prevents accurate measurements. ^cCO complexes may not be fully formed at 1.00-atm pressure; ϵ is an effective value for total [Fe^{II}].

Cu^{II}(HAPH) supports the N₅ coordination in the frozen glass. Cu(HAPH)⁺ has been isolated as the ClO₄⁻ salt from methanol; its crystal structure will be reported elsewhere.³⁷ The structure of Cu(HAPH)⁺ is a distorted square pyramid with an axial imidazole coordinated below the plane of the other N donors:



The frozen-glass (50:50 DMSO/H₂O) spectrum of Cu^{II}(HAPH) supports the N₃O donor set at pH = 3.50 in a square-planar array. The spectrum at pH = 9.56 is also rhombically distorted axial (Figure 1) ($g_{\parallel} = 2.22$, $g_{\perp} = 2.06$, $A_{\parallel} = 201 \times 10^{-4}$ cm⁻¹) compared to Cu^{II}(BLM)^{2,5,31} ($g_{\parallel} = 2.21$, $g_{\perp} = 2.06$, $A_{\parallel} = 188 \times 10^{-4}$ cm⁻¹) and Cu^{II}(AMPHIS)⁶ ($g_{\parallel} = 2.21$, $g_{\perp} = 2.05$, $A_{\parallel} = 183 \times 10^{-4}$ cm⁻¹). The combined evidence of the changes in the UV-visible spectra and the ESR spectra indicate an N₃O donor set at pH ≈ 3 and an N₄ or N₅ donor set above pH ≈ 7, both species having pseudo-square-planar or square-pyramidal coordination. The presence of DMSO (1:1 with H₂O), ethylene glycol (2:1 with H₂O), or CH₃OH (1:1 with H₂O) produced a spectral shift. When the Cu^{II}(HAPH) aqueous solution was adjusted to desired pH values, the spectra showed maxima at 630 nm (pH = 3.50) and 570 nm (pH = 9.06–11.18) as reported above. Addition of one of the other pure solvents for the purposes of making suitable frozen glasses for ESR study shifted the solution color from bluish purple in the pH = 9.06 and 11.18 solutions back to pale blue: 627 nm in DMSO (pH*¹⁸ = 9.06) and 620 nm in ethylene glycol (pH* = 5.59). The influence of the second solvent could be reversed by increasing the percent composition of H₂O. The best explanation for this phenomenon is the greater donor strength of DMSO, ethylene glycol, and methanol compared to that of water. Similar shifts are seen in the Cu^{II} complexes of Pypep³⁴ but not for the 5-coordinate

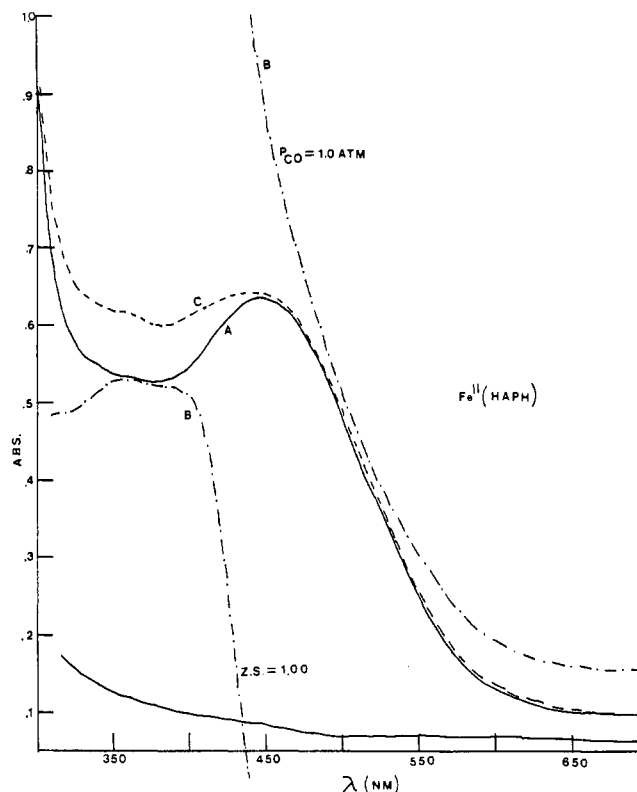


Figure 2. UV-visible spectra of Fe^{II}(HAPH) and Fe^{II}(HAPH)CO complexes (1.00-cm cells): (A) [Fe^{II}(HAPH)] = 2.00×10^{-3} M, pH = 7.57, $T = 21$ °C under 1 atm of Ar (tangerine solution); (B) [Fe^{II}(HAPH)CO] = 2.00×10^{-3} M with 1.0 atm of CO for 15 min, pH = 7.75 saturated (yellow solution); (C) sample B flushed with Ar gas for 12 min.

Cu(PMA)⁺ complex.⁴⁰ The appearance of the extra ESR feature above $g = 2.01$ at pH = 9.56 suggests at least some of the Cu^{II}(HAPH) species are in the N₅ donor environment similar to that of Cu^{II}(BLM) in the frozen glass even though only the N₄ donor environment is implicated in room-temperature solutions according to the electronic spectra for Cu^{II}(HAPH).

Fe^{II}(HAPH), Fe^{II}(HAPH)CO, and Related Complexes. Fe^{II} derivatives of HAPH, SAPH-3, SAPH-1, and BLM were prepared under Ar with Fe(NH₄)₂(SO₄)₂·6H₂O as the limiting reagent. The UV-visible spectral parameters for these complexes are given in Table I. This method reproduced the literature values for Fe^{II}(BLM).² All of these complexes showed the formation of a complex with amide deprotonation occurring with a pK_a value of ca. 6.0 compared to 5.2 for Fe^{II}(BLM).^{3c,45} In particular, the pK_a value for Fe^{II}(HAPH) was determined by potentiometric titration under Ar. A value of 6.50 ± 0.07 was obtained, which indicates that the amide pK_a values were identical for the Cu^{II} and Fe^{II} derivatives. The similarity of the visible spectra for Fe^{II}(HAPH), Fe^{II}(BLM), and Fe^{II}(SAPH-3) with respective bands at 445, 465, and 475 nm of comparable intensity ($\epsilon = (1.3\text{--}3.8) \times 10^2$ M⁻¹ cm⁻¹) strongly supports a common coordination for HAPH and BLM with Fe^{II}. N₅ donation has been proposed for BLM.^{4a,7,40,46}

An N₄O set for SAPH-1 and N₅S for SAPH-3 derivatives exists at a pH of about 8.0.⁸ The order of increasing ligand field energies HAPH > BLM ≈ PYML > SAPH-3 ≈ SAPH-1 is in keeping with imidazole coordination in the axial position for Fe^{II}(HAPH); the pH dependence infers the presence of deprotonated amide.

(46) The authors of ref 4a have argued for displacement of the amide-Fe^{II} bond in the Fe^{II}(BLM)CO complex. However, a careful examination of the ¹H NMR data in this reference more reasonably accommodates loss of the terminal primary amine and retention of the coordinated amide unit.

(47) Kurosaki, H.; Anan, H.; Kimura, E. *Nippon Kagaku Kaishi* **1988**, 691.

(48) Abbreviations: DMPO = 5,5-dimethyl-1-pyrroline N-oxide; PBN = α -phenyl-N-tert-butyl nitrene; PypepH = N-(2-(4-imidazolyl)ethyl)pyridine-2-carboxamide.

(49) Zhang, S.; Shepherd, R. E. *Inorg. Chem.* **1988**, *27*, 4712.

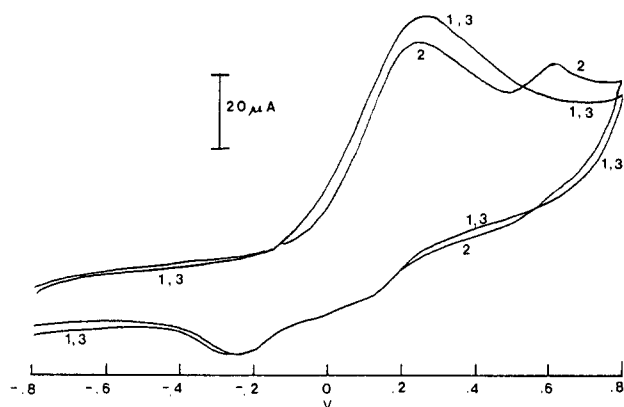
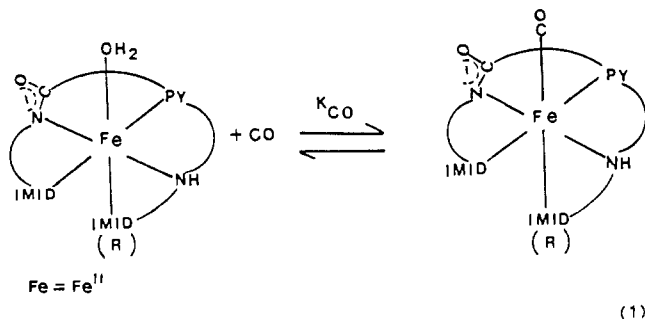


Figure 3. Cyclic voltammograms of $\text{Fe}^{\text{II}}(\text{HAPH})$ and $\text{Fe}^{\text{II}}(\text{HAPH})\text{CO}$ ($[\text{Fe}^{\text{II}}(\text{HAPH})] = 4.09 \times 10^{-3} \text{ M}$, $[\text{HAPH}]_{\text{tot}} = 4.93 \times 10^{-3} \text{ M}$, $\mu = 0.10 \text{ M NaClO}_4 + 0.10 \text{ M NaCl}$, $T = 22 \text{ }^\circ\text{C}$): (1) before saturation with CO gas; (2) after bubbling CO gas for 14 min; (3) after N_2 purge for 20 min. CV sweeps are at 100 mV/s .

If the imidazole moiety proposed for the axial site were pendant, the complex should behave nearly equivalently to $\text{Fe}^{\text{II}}(\text{SAPH-1})$ in its reaction with O_2 . $\text{Fe}^{\text{II}}(\text{SAPH-1})$ is very inefficient in generating trappable oxygen radicals upon autoxidation, while $\text{Fe}^{\text{II}}(\text{HAPH})$ is very efficient (see below).⁸⁻¹⁰ This implicates a different axial donor for $\text{Fe}^{\text{II}}(\text{HAPH})$, which cannot be the solvent; therefore, the axial site must involve the imidazole functionality. The most probable coordination about the Fe^{II} center would be a structure similar to that of $\text{Cu}^{\text{II}}(\text{HAPH})^{+37}$ with an additional solvent position coordinated in the second axial site of $\text{Fe}^{\text{II}}(\text{HAPH})$. The spectrum of $\text{Fe}^{\text{II}}(\text{HAPH})$ is shown in Figure 2A at $\text{pH} = 7.57$, where amide coordination is nearly complete. On the basis of the similarity of the spectrum of the $\text{Fe}^{\text{II}}(\text{BLM})$ complex, where axial coordination of an amide is proposed,^{2,39} one can assign an approximately octahedral coordination of the Fe^{II} center. The presence of a labile coordination site is shown by the ability of $\text{Fe}^{\text{II}}(\text{HAPH})$ to coordinate CO (Figure 2B) at 1.00-atm pressure. The new flat maximum feature in the 350–400-nm region ($\epsilon_{\text{eff}} = 707 \text{ M}^{-1} \text{ cm}^{-1}$) is similar to the ones of low-spin $\text{Fe}^{\text{II}}(\text{BLM})\text{CO}$ and $\text{Fe}^{\text{II}}(\text{PYML})\text{CO}$ adducts.^{1,4,5,39,46} The CO complexes are biochemically relevant species, as Burger, Peisach, et al. have shown that the $\text{Fe}^{\text{II}}(\text{BLM})\text{CO}$ complex has a spectrum similar to that of the first dioxygen intermediate (presumed to be $\text{Fe}^{\text{II}}(\text{BLM})(\text{O}_2)$) formed on addition of O_2 to $\text{Fe}^{\text{II}}(\text{BLM})$.⁴¹ The similarity in spectra of $\text{Fe}^{\text{II}}(\text{HAPH})\text{CO}$ and $\text{Fe}^{\text{II}}(\text{BLM})\text{CO}$ is added evidence for nearly identical donor sets in ligand field terms for the two complexes.⁴⁶

This equilibrium (eq 1) is fully reversible by purging the system with Ar gas. In 12.0 min ($4.5 t_{1/2}$) the spectrum is returned to



94.5% of the spectrum for the parent $\text{Fe}^{\text{II}}(\text{HAPH})$ complex. Only a hint of the remaining $\text{Fe}^{\text{II}}(\text{HAPH})\text{CO}$ complex is detected by a small residual absorbance at 350 nm (Figure 2C). The $E_{1/2}$ potential for $\text{Fe}(\text{HAPH})\text{CO}$ was determined from cyclic voltammetric studies (Figure 3) as 0.822 V (see Experimental Section). The rate of dissociation of the complex at $21 \text{ }^\circ\text{C}$ was measured by determining the time required to achieve complete recovery of $\text{Fe}^{\text{II}}(\text{HAPH})$; $k_d = (4.3 \pm 0.4) \times 10^{-3} \text{ s}^{-1}$. The substitution rate was estimated from the disappearance of the tangerine

$\text{Fe}^{\text{II}}(\text{HAPH})$ solution under saturated CO at 1.0 atm. Reaction was complete in 5.0 min ($t_{1/2} = 30.0 \pm 3.0 \text{ s}$). The solubility of CO is $9.96 \times 10^{-4} \text{ M}$. $[\text{Fe}^{\text{II}}(\text{HAPH})]_i$ was $2.00 \times 10^{-3} \text{ M}$. Assuming second-order kinetics for the forward coordination reaction in eq 1, the formation of the CO complex will obey pseudo-first-order kinetics with constant saturation by CO gas. The value of k_f is approximately $23.2 \pm 2.5 \text{ M}^{-1} \text{ s}^{-1}$, which combines with the reverse rate constant to give an estimate of K_{CO} for $\text{Fe}^{\text{II}}(\text{HAPH})$ of $(5.4 \pm 1.2) \times 10^3 \text{ M}^{-1}$. Under these conditions, the final solution is only $84.5 \pm 3.0\%$ coordinated at 1.00 atm of CO; $\epsilon_{400} = 837 \pm 30 \text{ M}^{-1} \text{ cm}^{-1}$ (corrected).

Related experiments were carried out with $\text{Fe}^{\text{II}}(\text{SAPH-3})$ (Figure SM2) and $\text{Fe}^{\text{II}}(\text{BLM})$ (Figure SM3). Both species form the CO complex as shown by the change from the original species with axial H_2O coordination (Figures SM2A and SM3A) to the $\text{Fe}^{\text{II}}(\text{SAPH-3})\text{CO}$ and $\text{Fe}^{\text{II}}(\text{BLM})\text{CO}$ complexes (Figures SM2B and SM3B, respectively). The $\text{Fe}^{\text{II}}(\text{BLM})\text{CO}$ complex has been previously reported in the literature.^{2,4,5} Both $\text{Fe}^{\text{II}}(\text{SAPH-3})\text{CO}$ and $\text{Fe}^{\text{II}}(\text{BLM})\text{CO}$ reverted to the original species upon purging with Ar (Figures SM2C and SM3C).

When $8.51 \times 10^{-4} \text{ M Fe}^{\text{II}}(\text{BLM})\text{CO}$ solution in 0.071 M NaCl was examined under N_2 by differential pulse procedures, two waves were observed: one at 0.176 V and another at +0.937 V vs NHE. The wave at +0.937 V decreased in amplitude with the increase in the +0.176-V wave upon purging with N_2 . The latter is the same wave as for $\text{Fe}^{\text{II}}(\text{BLM})$ without CO present.⁵⁰

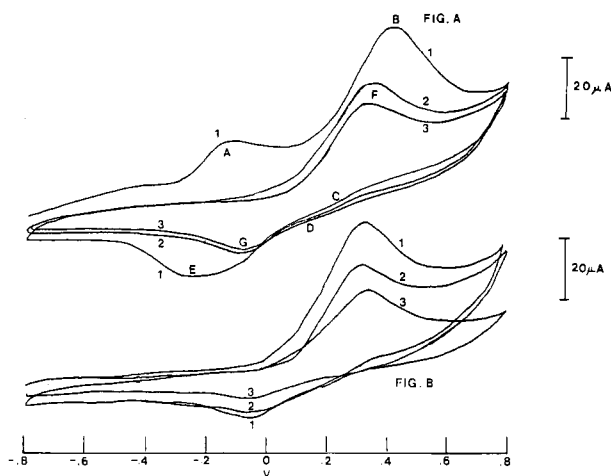
The rates for loss of CO from $\text{Fe}^{\text{II}}(\text{SAPH-3})\text{CO}$ and $\text{Fe}^{\text{II}}(\text{BLM})\text{CO}$ were determined to be ca. $(9.6 \pm 0.9) \times 10^{-3}$ and $(7.7 \pm 0.8) \times 10^{-3} \text{ s}^{-1}$ by the spectrophotometric procedures described for $\text{Fe}^{\text{II}}(\text{HAPH})\text{CO}$. Since all of the complexes added CO at $24 \pm 4 \text{ M}^{-1} \text{ s}^{-1}$, the formation constants, K_{CO} , will be nearly the same: 2.6×10^3 , 3.2×10^3 , and 5.4×10^3 for the SAPH-3, BLM, and HAPH complexes, respectively. The weakest interaction for $\text{Fe}^{\text{II}}(\text{SAPH-3})$ has the poorest trans axial donor (H_2O or RS^-) compared to the N-donors of HAPH and BLM. Similar relationships concerning the donation by axial bases on CO affinities are known for the Fe^{II} porphyrin.^{32,33}

Electrochemical Studies by Cyclic Voltammetry. Cyclic voltammograms for the $\text{Fe}^{\text{II}}(\text{HAP})$ and $\text{Fe}^{\text{II}}(\text{HAPH})$ systems were obtained in 0.10 M NaClO_4 at $22 \text{ }^\circ\text{C}$ under Ar. A 0.10 M $\text{NaClO}_4/0.10 \text{ M NaCl}$ mixture was also studied for $\text{Fe}^{\text{II}}(\text{HAPH})$ to examine the influence of Cl^- on the $E_{1/2}$ value. Cyclic voltammograms of $6.69 \times 10^{-3} \text{ M Fe}(\text{NH}_4)_2(\text{SO}_4)_2 \cdot 6\text{H}_2\text{O}$ were also observed at pH values of 4.37, 6.72, and 8.23. These serve as blank voltammograms (not shown) for the purpose of evaluating the extent of chelation by HAP and HAPH to Fe^{II} . $\text{Fe}^{\text{II}}(\text{HAP})$ was not coordinated at $\text{pH} = 3.03$ but is fully coordinated above $\text{pH} \approx 4.5$. The solution is light yellow for the $\text{Fe}^{\text{II}}(\text{HAP})$ complex. $\text{Fe}^{\text{II}}(\text{HAPH})$ appears to be partially coordinated even at $\text{pH} \approx 3$, where the solution is rose-colored, changing to dusty rose at $\text{pH} = 4.0$ –5.5, orange at $\text{pH} \approx 7$ in 0.10 M NaClO_4 or tangerine with 0.10 M NaCl present, and darker orange at $\text{pH} \approx 8$; an additional reddish brown or rose-orange transitory species also forms with localized addition of NaOH at $\text{pH} \approx 8$ –9 and increases in abundance above $\text{pH} = 10$. The $\text{p}K_a$ value of the amide NH was determined to be 6.50 ± 0.07 from a potentiometric titration ($T = 22 \text{ }^\circ\text{C}$, $\mu = 0.05$), the same value as observed for $\text{Cu}^{\text{II}}(\text{HAPH})$. This assists in assignment of the most probable donor set for each of the four $\text{Fe}^{\text{II}}(\text{HAPH})$ species. The reddish brown form at high pH (8–9), formed by localized concentration effects upon HO^- addition, relaxes slowly to the darker orange form. None of the cyclic voltammograms of $\text{Fe}^{\text{II}}(\text{HAP})$ above $\text{pH} = 4$ or of $\text{Fe}^{\text{II}}(\text{HAPH})$ above $\text{pH} = 2$ were the same as from $\text{Fe}^{\text{II}}(\text{HAPH})$ solution under saturated CO at 1.0 atm. Reaction was complete in 5.0 min ($t_{1/2} = 30.0 \pm 3.0 \text{ s}$). The solubility of CO is $9.96 \times 10^{-4} \text{ M}$. $[\text{Fe}^{\text{II}}(\text{HAPH})]_i$ was $2.00 \times 10^{-3} \text{ M}$. Assuming second-order kinetics for the forward coordination reaction in eq 1, the formation of the CO complex will obey pseudo-first-order kinetics with constant saturation by CO gas. The value of k_f is approximately $23.2 \pm 2.5 \text{ M}^{-1} \text{ s}^{-1}$, which combines with the reverse rate constant to give an estimate of K_{CO} for $\text{Fe}^{\text{II}}(\text{HAPH})$ of $(5.4 \pm 1.2) \times 10^3 \text{ M}^{-1}$. Under these conditions, the final solution is only $84.5 \pm 3.0\%$ coordinated at 1.00 atm of CO; $\epsilon_{400} = 837 \pm 30 \text{ M}^{-1} \text{ cm}^{-1}$ (corrected).

(50) In 0.10 M NaCl the differential pulse peak of $\text{Fe}^{\text{II/III}}(\text{BLM})$ shifts to a final value of +0.177 V. This value is in reasonable agreement with an $\text{Fe}^{\text{II/III}}(\text{BLM})$ $E_{1/2}$ value of 0.13 V measured by a half-titration procedure.²² Experiments carried out for $\text{Fe}(\text{HAPH})$ show the 0.10 M NaClO_4 solutions give potentials ca. 0.06 V less positive than when 0.10 M NaClO_4 plus 0.10 M NaCl was present. The additional shift suggests axial coordination of Cl^- . Application of the correction to the half-wave potential gives an $E_{1/2}$ value of 0.12 V in agreement with titration results. See also ref 52.

Table II. Cyclic Voltammograms for Fe^{II}(HAP) and Fe^{II}(HAPH)

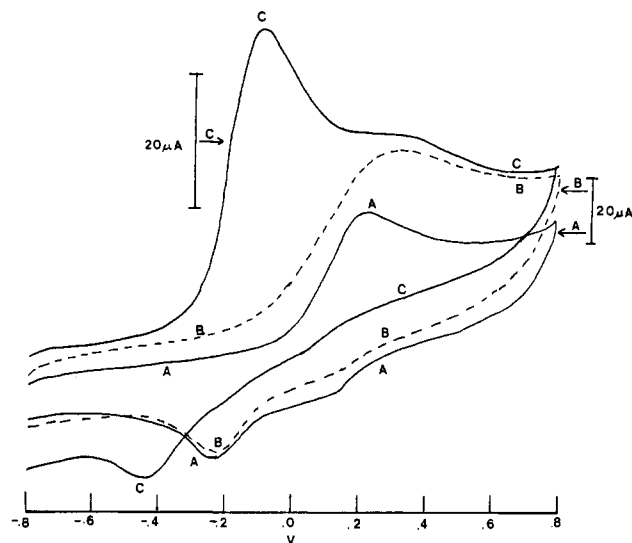
| pH | soln color, complex | $E_{1/2}$, V vs NHE |
|---|--|-----------------------------|
| $\mu = 0.10$ M NaClO ₄ | | |
| 5.01 | lt yellow, Fe ^{II} (HAP) | 0.48 |
| 8.10 | yellow, Fe ^{II} (HAP) | 0.632, 0.072 |
| 2.10 | dirty pink, Fe ^{II} (HAPH) | 0.32 |
| 4.10 | dusty rose, Fe ^{II} (HAPH) | 0.47 |
| 7.00 | orange, Fe ^{II} (HAPH) | 0.407 |
| 8.70 | reddish brown, Fe ^{II} (HAPH) | 0.092 (major), 0.40 (minor) |
| $\mu = 0.10$ M NaClO ₄ + 0.10 M NaCl | | |
| 4.20 | dusty rose, Fe ^{II} (HAPH) | 0.492 |
| 6.01 | orange, Fe ^{II} (HAPH) | 0.452 |
| 7.20 | tangerine, Fe ^{II} (HAPH) | 0.457 |
| 7.10 | bright yellow, Fe ^{II} (HAPH)CO | 0.822 |
| $\mu = 0.10$ M Phosphate Buffer | | |
| 6.86 | dark orange, Fe ^{II} (HAPH) | 0.067 |
| 6.86 | orange, Fe ^{II} (BLM) | 0.092 |

**Figure 4.** Cyclic voltammograms of Fe^{II}(HAP): (A) pH = 8.1, [Fe^{II}(HAP)] = 6.60 × 10⁻³ M, $\mu = 0.10$ M NaClO₄, $T = 22$ °C, CV sweep at 100 mV/s, (1) first scan, (2) second continuous scan, (3) third continuous scan; (B) pH = 5.01, other conditions same as in (A).

(NH₄)₂(SO₄)₂·6H₂O blank voltammograms in similar media at a given pH. The half-wave potentials are summarized in Table II.

The cyclic voltammogram of Fe^{II}(HAP) is shown in Figure 4. The pH = 5 form is shown in Figure 4B. Only one oxidation wave but two reduction waves are observed, together with decreasing amplitudes of all waves with each 16-s complete cycle. The evidence supports demetalation from the Fe^{III} form of Fe(HAP). One reduction wave corresponds to the reversible complementary wave, while the more prominent reduction wave represents a partially unwrapped or hydrolyzed form of Fe^{III}(HAP). Hydrolysis and precipitation of iron hydroxides from the electrode monolayer slowly removes the Fe^{III} species, resulting in loss of current amplitude in sweeps 1–3. At pH = 8.10 (Figure 4A) the system is further complicated by two forms of the Fe^{II}(HAP) species which are not at equilibrium. Two distinctly different forms exhibit a large difference in oxidation wave potentials at positions A and B in Figure 4A. After the first 72 s, the species giving rise to waves A and E is destroyed, leaving only the species like the one detected for Fe^{II}(HAP) at pH = 5.01. The reduction wave shows at least three different species (C, D, and E on sweep 1). Reduction C appears to be the reversible wave for B. Successive scans adopt the pattern with waves at F, C, and G that match those of Fe^{II}(HAP) at pH = 5.01.

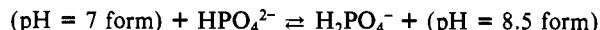
The most important aspect of the Fe^{II}(HAP) cyclic voltammogram is that the N₃O₃ donor set produces a complex with an $E_{1/2}$ value near 0.63 V, which is higher than for any species observed above pH ≈ 4 with Fe^{II}(HAPH). The $E_{1/2}$ values for Fe^{II} complexes with sp³ N-donors generally decrease with increasing numbers of N-donating ligands.³⁴ Also note that the $E_{1/2}$ value for Fe^{II}(BLM) with an N₅O donor set is 0.13 V.^{22,50,51,52}

**Figure 5.** Cyclic voltammograms of Fe^{II}(HAPH) ([Fe^{II}(HAPH)] = 4.09 × 10⁻³ M, [HAPH]_{tot} = 4.93 × 10⁻³ M, $T = 22$ °C, CV sweeps at 100 mV/s): (A) $\mu = 0.10$ M NaClO₄, pH = 7.00; (B) $\mu = 0.10$ M NaClO₄ + 0.10 M NaCl, pH = 7.20; (C) $\mu = 0.10$ M NaClO₄, pH = 8.70.

The cyclic voltammograms for Fe^{II}(HAPH) are shown in Figure 5: part A, pH = 7.00, 0.10 M NaClO₄; part B, pH = 7.20, 0.10 M NaClO₄/0.10 M NaCl; part C, pH = 8.70, 0.10 M NaClO₄. The $E_{1/2}$ potential for the dominant species at pH = 8.70 in Figure 5C has an $E_{1/2}$ value of 0.092 V, which is quite similar to that for Fe^{II}(BLM). The pK_a value of 6.50 ± 0.07 for the amide donor implicates significant coordination of the amide group in all voltammograms in Figure 5. The higher $E_{1/2}$ value at pH = 4.10 and the distinct color change from dusty rose at 4.10 to orange at 7.00 following amide deprotonation implicates a structure at pH = 7 significantly different from the pH = 4 form. Yet the yellow color of the Fe^{II}(HAP) complex (N₃O₃) is different from that of Fe^{II}(HAPH) at pH = 4, indicating more than three N donors for Fe^{II}(HAPH), even at pH = 4, than found for Fe^{II}(HAP). Thus, the donor set appears to be bounded by the following pH conditions for Fe^{II}(HAPH):

| | | | | |
|--|---|--|---|---|
| pH 4, N ₄ dusty rose (no amide donor) $E_{1/2} = 0.47$ V | → | pH 7, N ₄ orange (amide coordinated) $E_{1/2} = 0.407$ V | → | pH ≥ 8.5, N ₅ dark orange (amide coordinated) $E_{1/2} = 0.092$ V |
|--|---|--|---|---|

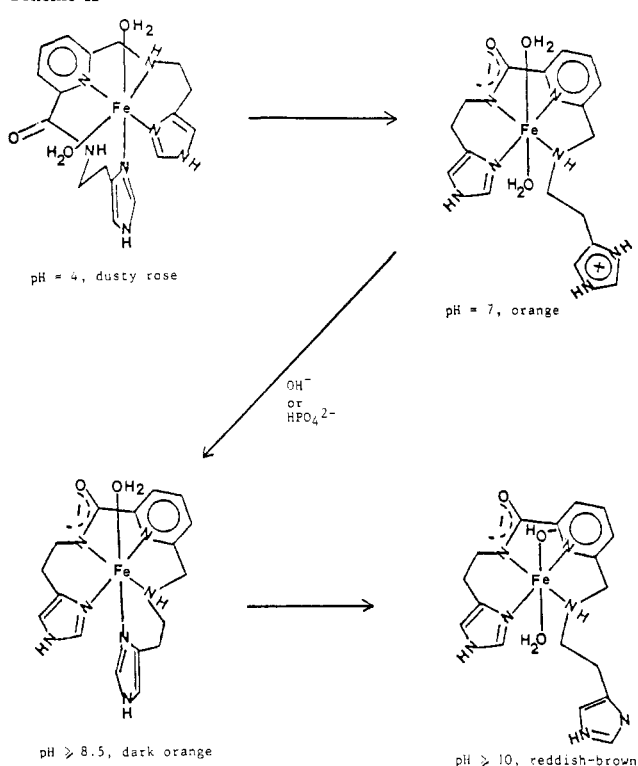
In the presence of phosphate buffer at pH = 6.86, the dark orange form is stabilized ($E_{1/2} = 0.067$ V by DP method). This implicates the equilibrium



The presence of Cl⁻ in the medium causes a small positive shift of ca. 0.06 V on the potential of Fe^{II}(HAPH) at pH = 7.0, which suggests axial association of Cl⁻, but the shift cannot account for the major 0.315-V decrease at pH = 8.5 for the dark orange form. The orange color of the pH = 7 form suggests a structure related to that of the pH = 8.5 form, and the species must contain a protonated group that can transfer protons to HPO₄²⁻ (e.g. the

- (51) Demetalations of the Fe^{III} complexes of BLM, SAPH-3, and HAPH have been noted previously.^{8,10,41} The demetalation process is sensitive to both pH and counterions.^{8,10,41} Fe^{III}(HAPH), formed by the O₂ oxidation of Fe^{II}(HAPH), begins to demetallate as Fe₂(HPO₄)₃ within 60 s in phosphate buffer but only after 20–25 min as ferric hydroxide in unbuffered 0.10 M NaCl solution at pH ≈ 7. Both precipitates were characterized by IR spectra vs those of authentic samples. The differential pulse method is sufficiently rapid to avoid complication of the instability of the Fe^{III} complexes in obtaining $E_{1/2}$ values. Therefore, the corrected value of +0.12 V appears to be the most reliable value for the Fe^{III}/II(BLM) couple.
- (52) Van Atta, R. B.; Long, E. C.; Hecht, S. M.; van der Marel, G. A.; van Boom, J. H. *J. Am. Chem. Soc.* 1989, 111, 2722. These authors report an $E_{1/2}$ value of 0.12 V in 0.05 M cacodylate buffer for Fe^{III}/II(BLM).

Scheme II



moiety has $pK_a \approx 7$). The sequence of structural changes compatible with ligand field changes, the $E_{1/2}$ values, and the dependence on HPO_4^{2-} is as shown in Scheme II. Species analogous to the $\text{pH} = 7$ form and $\text{pH} = 8.5$ form have been identified by Kimura et al. for the Fe^{II} complex of his "L₂" ligand, which differs from HAPH only by a terminal $\text{CH}_2\text{CH}(\text{CONH}_2)\text{NH}_2$ moiety replacing the axial histidyl unit of HAPH.⁴⁷

As was seen for the $\text{Fe}^{\text{II}}(\text{HAP})$ complex, repetitive cyclic voltammetric scans (not shown in Figure 5) implicated ligand unwrapping and eventual demetalation from the Fe^{III} complexes.⁵¹ On the first reduction cycle in Figure 5A only 30% of the reversible $\text{Fe}^{\text{III}}(\text{HAPH})$ species is recovered while 70% is reduced at a more negative potential. The half-time for loss of the electrochemically reversible wave gives an estimate of the rate of ligand unwrapping of $\text{Fe}^{\text{III}}(\text{HAPH})$ at $\text{pH} = 7.0$ of $9.6 \times 10^{-2} \text{ s}^{-1}$.

$\text{Fe}^{\text{II}}(\text{HAPH})/\text{O}_2$ Reaction. The ability of $\text{Fe}^{\text{II}}(\text{HAPH})$ to activate O_2 was assessed by the spin-trapping technique^{14,25} using the DMPO spin trap at 0.24 M. The high spin trap concentration was shown in a series of trial experiments to be essential in trapping a sufficient radical concentration with $\text{Fe}^{\text{II}}(\text{BLM})$ or its analogues. A 20-fold lower $[\text{DMPO}]$ (0.012 M) effectively traps HO^\bullet generated via the $\text{Fe}(\text{edta})^{2-}/\text{H}_2\text{O}_2$ reaction.¹⁴ A 1.00-mL solution of 0.72 M DMPO was rapidly bubbled with O_2 gas while a suitable 2.00-mL sample in the range 1.49×10^{-3} – 2.24×10^{-3} M $\text{Fe}^{\text{II}}(\text{HAPH})$ or $\text{Fe}^{\text{II}}(\text{BLM})$ was prepared under Ar as described previously. The Fe^{II} complex was injected into the O_2 -saturated solution with continuous rapid O_2 bubbling. $[\text{Fe}^{\text{II}}]_i$ was 1.00×10^{-3} – 1.50×10^{-3} M and $[\text{DMPO}] = 0.24$ M after mixing. The solutions changed from red-orange ($\text{Fe}^{\text{II}}(\text{BLM})$) or tangerine ($\text{Fe}^{\text{II}}(\text{HAPH})$) to yellow in the first 10 s. Oxygenation was continued for another 15 s.

An ESR flat cell was filled and mounted in the microwave cavity of a Varian E-4 EPR instrument. Tuning at 9.482 GHz required about 30 s. The first scan for the $\text{Fe}^{\text{II}}(\text{BLM})$ system showed the presence of both $\text{HO}_2(\text{DMPO})^\bullet$ and $\text{HO}(\text{DMPO})^\bullet$. Nearly identical amplitudes were observed for different trials, one with BLM in 20% excess and the other with Fe^{II} in excess (Figure 6A,B). The signal for $\text{HO}_2(\text{DMPO})^\bullet$ (shown by arrows) vanished within the first 2.0 min of scanning time (ca. 3 min after injection) to yield the final constant $\text{HO}(\text{DMPO})^\bullet$ signal in Figure 6C. The presence of a large excess of BLM leads to a great number of carbon-centered radical signals in about 25 min. Therefore, the

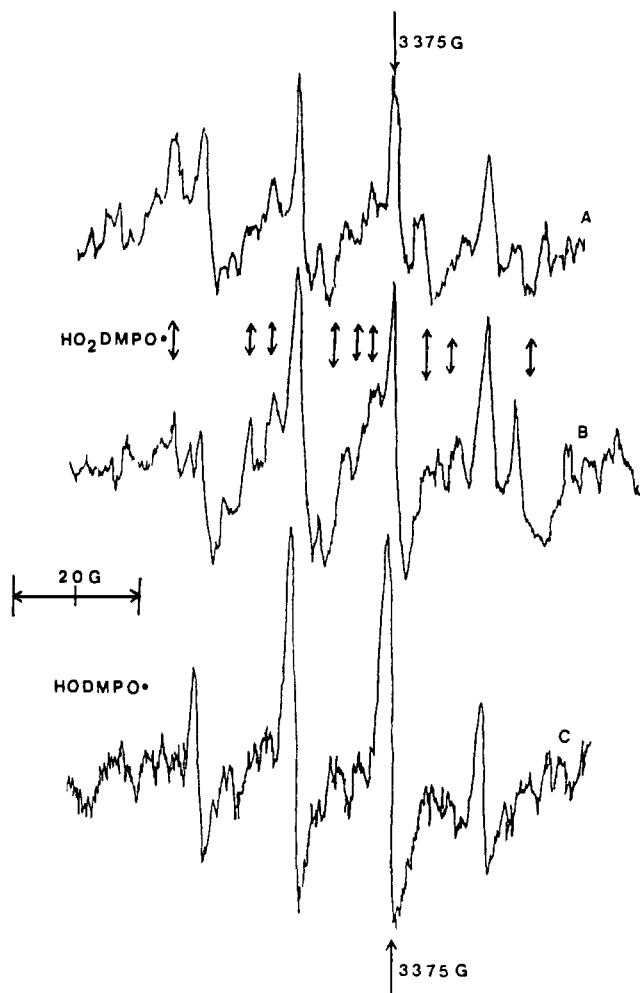


Figure 6. $\text{Fe}^{\text{II}}(\text{BLM})$ spin-trapping studies with 0.24 M DMPO: (A) $[\text{Fe}^{\text{II}}(\text{BLM})]_i = 1.25 \times 10^{-3}$ M, O_2 saturated, $\text{pH} = 7.35$, excess $\text{Fe}^{\text{II}} = 7.5 \times 10^{-4}$ M, $\text{RG} = 8 \times 10^4$; (B) $[\text{Fe}^{\text{II}}(\text{BLM})]_i = 1.00 \times 10^{-3}$ M, O_2 saturated, $\text{pH} = 8.00$, $[\text{excess BLM}] = 2.0 \times 10^{-4}$ M, $\text{RG} = 8 \times 10^4$; (C) solution A at 9.3 min.

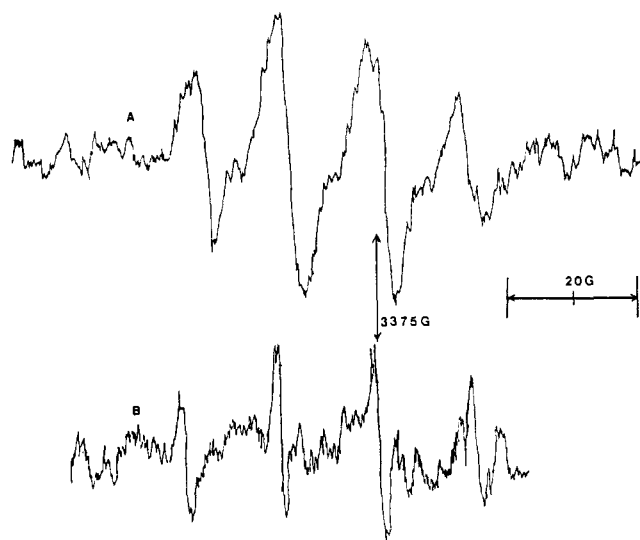


Figure 7. $\text{Fe}^{\text{II}}(\text{HAPH})$ spin-trapping studies with 0.24 M DMPO: (A) $[\text{Fe}^{\text{II}}(\text{HAPH})]_i = 8.33 \times 10^{-4}$ M, $[\text{H}_2\text{O}_2] = 0.49$ M, $\text{pH} = 7.50$, $\text{RG} = 5 \times 10^4$; (B) $[\text{Fe}^{\text{II}}(\text{HAPH})]_i = 1.34 \times 10^{-3}$, O_2 saturated, $\text{pH} = 7.50$, $\text{RG} = 8 \times 10^4$. ESR settings: 9.482 GHz, 1.60-G modulation amplitude 15.0-mW power, 3.0-s time constants, 8.0-min sweep rate.

yield of HO^\bullet was evaluated from the more stable system with Fe^{II} in slight excess. $\text{Fe}^{\text{II}}/\text{O}_2/\text{DMPO}$ alone does not generate comparable signals. $\text{Fe}^{\text{II}}(\text{HAPH})$ was studied with both O_2 and H_2O_2

as the oxidant. The O₂ reaction was at O₂ saturation while the H₂O₂ concentration was made 0.49 M. The HO(DMPO)[•] signals that were obtained with Fe^{II}(HAPH) and H₂O₂ are seen in Figure 7A and those with O₂ in Figure 7B. When the amplitudes of the second- or third-derivative lines of HO(DMPO)[•] are compared and scaled for differences in receiver gain settings, molar amounts of Fe^{II} present, and the 3e required to form one HO[•] from O₂ vs 1e per HO[•] from H₂O₂, it is observed that Fe^{II}(HAPH) is 53% as efficient as Fe^{II}(BLM) in HO[•] generation via O₂. The H₂O₂ oxidation of Fe^{II}(HAPH) is 63% as efficient as the Fe^{II}(BLM)/O₂ system. The absolute magnitudes of these numbers may vary slightly with O₂ flow rate and the total initial Fe^{II} concentrations because the species being trapped are reducible by Fe^{II} competitively. However, under very similar initial Fe^{II} concentrations and virtually identical procedures of mixing, these results show that Fe^{II}(HAPH) has a reactivity with O₂ very comparable to that of Fe^{II}(BLM).

Conclusions. Both the Fe^{II}(HAPH) and Cu^{II}(HAPH) complexes behave similarly to their Fe^{II}(BLM) and Cu^{II}(BLM) counterparts. Very similar ESR and electronic spectra have been found for Fe^{II} and Cu^{II} HAPH complexes compared to the BLM, PYML, and AMPHIS chelates and Kimura's "L₂" ligand.⁴⁷ The pH = 7 form of Fe^{II}(HAPH) appears to be the same as one of the N₄ isomers for Cu^{II}, but the additional evidence of a protonated imidazole with pK_a ≈ 7.8 is suggested from an equilibrium shift with HPO₄²⁻ present and by a slight break in the potentiometric titration curve of Fe^{II}(HAPH). The cyclic voltammetry clearly shows axial coordination at pH ≥ 8.5 for Fe^{II}(HAPH).

Synthesis of the HAPH ligand and its Fe^{II}(HAPH) complex provides a hybrid molecule between the BLM core donors and those of the heme and cytochrome metalloproteins^{2a} which have an axial imidazole (histidine) donor. Like the Fe^{II} hemes,

Fe^{II}(HAPH) binds CO. The Fe^{II}(HAPH) complex also reacts with O₂. It forms O₂⁻, reduced to HO[•] in yields of 53% of that for Fe^{II}(BLM) under spin-trapping conditions. Both Fe^{II}(HAPH) and Fe^{II}(BLM) form CO complexes with comparable stabilities (K_f ≈ 5.4 × 10³ M⁻¹). This translates into a favorable free energy of back-donation of nearly 5.1 kcal/mol from the Fe^{II} center to CO. This is substantially less than the ~38.2 kcal/mol energy of back-donation of (NH₃)₅Ru²⁺ toward CO.²⁶⁻²⁸ The electrochemical data reveal a net 9.6 kcal favorability of the Fe^{II} state in the presence of CO (compared to axial H₂O). Assuming the CO complex is low spin, as the Fe^{II}(BLM)CO complex, and assuming the conversion high-spin Fe^{II} to low-spin Fe^{II} costs about 5.5 kcal/mol as estimated from stabilities of Fe^{II}(HS) imidazole vs those of Fe^{II}(LS) imidazole complexes,⁴³ there should be a net free energy released for binding CO of ~4.1 kcal/mol. This is in excellent agreement with the 5.1 kcal/mol estimated from the K_{CO} constant for formation of Fe(HAPH)CO⁺. The significant reactivity of the Fe^{II}(HAPH)/O₂ reaction has prompted further work in this laboratory to synthesize molecules containing the HAPH chelation moiety and related units for the purpose of antitumor drug design.

Acknowledgment. We gratefully acknowledge support under NSF Grant CHE-8417751 and the donors of the Petroleum Research Fund, administered by the American Chemical Society, for support of this work. We thank A. Marcus and J. F. Siuda for assistance in obtaining the HRMS data.

Supplementary Material Available: Visible spectra of the complexes Cu^{II}(HAPH) and Cu^{II}(BLM) (Figure SM-1), Fe^{II}(SAPH-3) and Fe^{II}(SAPH-3)CO (Figure SM-2), and Fe^{II}(BLM) and Fe^{II}(BLM)CO (Figure SM-3) and the FTIR spectrum of [Cu(HAPH)](ClO₄)·1.61H₂O (Figure SM-4) (4 pages). Ordering information is given on any current masthead page.

Contribution from the Department of Chemistry, University of Florence, Florence, Italy, and Institute of Agricultural Chemistry, University of Bologna, Bologna, Italy

Binding of Fluoride to Copper Zinc Superoxide Dismutase

L. Banci,[†] I. Bertini,^{*†} C. Luchinat,[‡] A. Scozzafava,[†] and P. Turano[†]

Received August 11, 1988

The interaction of fluoride with copper zinc superoxide dismutase (SOD) has been reinvestigated by using both bovine and yeast isoenzymes. The affinity of anions for the latter isoenzyme is larger, and this avoids much of the ionic strength effects connected with weak binding ligands. ¹⁹F NMR studies on fluoride in presence of yeast SOD confirm that the anion binds the copper ion. ¹H NMR studies of the Cu₂Co₂SOD derivatives in the presence of F⁻ indicate that no ligand is removed from coordination. Water ¹H NMR T₁⁻¹ measurements on solutions of Cu₂Zn₂SOD-fluoride indicate that exchangeable protons that feel the paramagnetic center are present. This unique behavior of fluoride has opened new perspectives on the understanding of anion binding to copper zinc SOD.

Introduction

The investigation of the binding of anions with copper zinc superoxide dismutase (SOD hereafter) has been a major field of interest¹⁻⁴ in the characterization of the enzyme because it can provide information on the catalytic mechanism, as superoxide itself is an anion.

Cyanide and azide were found to be competitive inhibitors⁵ whereas cyanate and thiocyanate do not inhibit the enzyme.⁶ The ionic strength has some effects on this fast reaction.⁷ The binding at the copper ion of CN⁻, N₃⁻, NCO⁻, and NCS⁻ has been shown by EPR, the spectrum of the enzyme being rhombic and the spectra of the adducts being essentially axial.¹⁻⁴ Sometimes the appearance of a charge-transfer band in the electronic spectra is also observed.⁸ We have investigated SOD and its derivatives through ¹H NMR spectroscopy on the cobalt-substituted derivative

(Cu₂Co₂SOD).⁹ The magnetic coupling between copper and cobalt¹⁰ makes the system suitable for ¹H NMR investigation. All the proton signals of the histidines bound to both cobalt and copper are observed well shifted outside the diamagnetic region.

- (1) Fee, J. A.; Gaber, B. P. *J. Biol. Chem.* **1972**, *247*, 60-65.
- (2) Fridovich, I. In *Advances in Inorganic Biochemistry*; Eichorn, G. L., Marzilli, L. G., Eds.; Elsevier: New York, 1979; Vol. 1, pp 67-90.
- (3) Fielden, E. M.; Rotilio, G. In *Copper Proteins and Copper Enzymes*; Lontie, R., Ed.; CRC: Boca Raton, FL, 1984; Vol. 2, pp 27-61.
- (4) Valentine, J. S.; Pantoliano, M. W. In *Copper Proteins*; Spiro, T. G., Ed.; Wiley: New York, 1981; Vol. 3, Chapter 8.
- (5) Rigo, A.; Stevanato, R.; Viglino, P.; Rotilio, G. *Biochem. Biophys. Res. Commun.* **1977**, *79*, 776-783.
- (6) Ozaki, S.; Hirose, J.; Kidani, Y. *Inorg. Chem.* **1988**, *27*, 3746-3751.
- (7) Cudd, A.; Fridovich, I. *J. Biol. Chem.* **1982**, *257*, 11443-11447.
- (8) Pantoliano, M. W.; Valentine, J. S.; Nafie, L. A. *J. Am. Chem. Soc.* **1982**, *104*, 6310-6317.
- (9) Bertini, I.; Lanini, G.; Luchinat, C.; Messori, L.; Monnanni, R.; Scozzafava, A. *J. Am. Chem. Soc.* **1985**, *107*, 4391-4396.
- (10) Morgenstern-Baradau, I.; Cocco, D.; Desideri, A.; Rotilio, G.; Jordanov, J.; Dupre, N. *J. Am. Chem. Soc.* **1986**, *108*, 300-302.

[†] University of Florence.

[‡] University of Bologna.